Catalysis Science & Technology

ROYAL SOCIETY OF CHEMISTRY

MINI REVIEW

View Article Online
View Journal | View Issue

Cite this: *Catal. Sci. Technol.*, 2021, 11, 43

Photocatalytic materials and light-driven continuous processes to remove emerging pharmaceutical pollutants from water and selectively close the carbon cycle

Gianvito Vilé

Pharmaceutical pollutants are increasingly being present in water effluents. Over the past decades, the emergence of advanced oxidation processes has provided a tool to catalytically remove organic pollutants and harmful pathogens. However, researchers have focused too often on increasing the degradation rate of the contaminants, without ensuring as well the formation of more biodegradable products. As a result, by-products that are more toxic than the initial substrate have frequently been formed, limiting the industrial and societal exploitation of this technology. In an attempt to urgently fill this gap, this minireview analyses in a holistic manner past and present technologies for water purification, outlining possible examples of ultraselective photocatalytic materials and reactor concepts to obtain biodegradable products. Based on the analysis conducted, guidelines for the rational design of catalytic materials and for the selection of emerging reactor concepts are put forward. We also highlight current technological barriers and future research needs that should be explored in greater depth in the quest for integrated and intensified continuous-flow operations.

Received 31st August 2020,
Accepted 23rd September 2020

DOI: 10.1039/d0cy01713b

rsc.li/catalysis

Emerging pharmaceutical contaminants and the water challenge

Among the greatest challenges mankind is facing, water scarcity and pathogen spread occupy a prominent role. It is well recognised that population growth, urbanization, industrial growth, and climate change are consuming Earth's resources at an unsustainable rate. And in the World Water Development Report 2019,[1] the United Nations have highlighted that the availability of clean water is becoming a matter of major concern in the world due to pollution. Untreated sewage, agricultural runoff, inadequately treated wastewater from municipal and industrial (chemical) plants, and consumption of medical (and illegal) drugs continue to deplete the quality of water, contaminating supply systems with micropollutants. These include pharmaceuticals and waterborne pathogens that were once thought to be under control but, due to changes in human demographics and increasing antimicrobial resistance, are reappearing and

Department of Chemistry, Materials, and Chemical Engineering "Giulio Natta", Politecnico di Milano, Piazza Leonardo da Vinci 32, IT-20133 Milano, Italy. E-mail: gianvito.vile@polimi.it

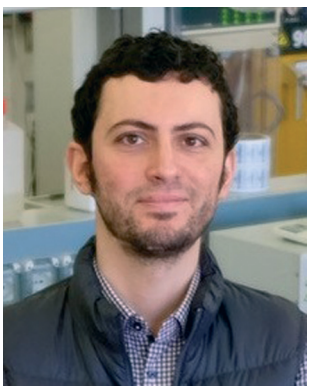

Gianvito Vilé

Dr. Gianvito Vilé studied Chemical Engineering at Politecnico di Milano (Italy) and was a visiting student at TU Delft (The Netherlands). In 2015, he obtained a PhD in Chemical Engineering in the group of Prof. Javier Pérez-Ramírez at ETH Zurich (Switzerland) with a thesis on the design of catalytic materials and flow reactors for selective hydrogenation. Then, he moved to industry, as a Lab Head at Idorsia Pharmaceuticals, where he was responsible for applying enabling technologies (i.e., flow chemistry, high-throughput synthesis, process intensification, single-site catalysis) to reactions encountered in drug discovery. In 2020, he returned to academia, accepting a faculty position at Politecnico di Milano (Italy). He is currently heading the Innovation Lab for Sustainable Process Intensification and his group is developing novel structured catalysts and reactor concept for the synthesis of pharmaceuticals and for the circular recovery of contaminants from water.

causing amplified incidence of infections.[2,3] Among those, protozoa such as *E. coli* and viruses such as *Norovirus*, *Rotavirus*, and *Reovirus* are particularly critical because they are difficult to detect in water sewage and resistant to all current disinfection/elimination technologies.[4]

Urban areas, with their capillary healthcare and industrial infrastructures, represent an incontestable release source of complex mixtures of active pharmaceutical ingredients and biological pollutants.[5] These substances and metabolites pass from humans, through toilets, into public wastewater plants, which are designed to reduce loads of carbon, nitrogen, and phosphorus of traditional non-polar chemical compounds, but are ineffective with polar and poorly-degradable species.[6]

Hospitals and pharmaceutical industries, in particular, are responsible for the release of thousands of potential contaminants. A recent study across Europe and the US has shown that pharmaceutical contamination in water is typically low (<100 ng L^{-1} per chemical) in most municipal areas,[7] but has a significantly higher extent (*ca.* 500 000 ng L^{-1}) in effluents close to manufacturing facilities.[8] It is important to recognize that in the US (and in many other high-income countries in Europe and Asia), strict good manufacturing practices are enforced; other parts of the world with less developed industrial and healthcare systems might be exposed to even higher levels of contamination. Hence, the problem of pharmaceutical contamination in water represents a huge public health concern. Table 1 includes a list of important pollutants based on field studies independently conducted by the US Environmental Protection Agency and the European Environment Agency.[9]

The problem is exacerbated by the fact that water is essential for life and water shortage is the fourth highest risk factor for burden of disease in Africa and the Middle East. By 2050, projections highlight that water scarcity will affect high-income countries such as the US, Portugal, Italy, Israel, Spain, Greece, Japan, and Australia (Fig. 1).[1] In this context, wastewater is gaining momentum as an alternative source of water, and scientists are starting to shift the paradigm of wastewater management from 'treatment and disposal' to 'recovery, reuse, and recycle'. Reclaimed water can help mitigate the damaging effects of local water scarcity and provide a source of water in seasons of shortage. Therefore, it is not surprising that the United Nations have declared the importance of meeting the wastewater challenge among the UN Sustainable Development Goals for our millennium,[1] calling for urgent, novel routes to remove emerging pollutants and recover chemicals from it.

Successes and pitfalls of wastewater treatment around the world

To effectively grasp the technological challenges encountered in removing emerging pollutants, it is key to first evaluate state-of-the-art processes and their limitations. The traditional municipal wastewater technology combines two basic stages.[10] In the primary step, solids are settled and removed by filtration. The secondary step uses bacteria to decompose organic matter under aerobic or anaerobic conditions. The type of biological treatment depends on several factors, including compliance with environmental regulations. A tertiary treatment might be possible, depending on the final utilization of the reclaimed water. Tertiary treatment is being increasingly applied in industrialized countries and the most common technologies are microfiltration or membrane separation. New environmental challenges, however, have placed fresh burdens on these types of wastewater systems. Today's pollutants are more difficult to remove (as they are poorly-degradable).[4]

Advanced wastewater treatment plants have been developed and the gold standard of such technologies combines physical and chemical unit operations. This system was implemented for the first time in California, replicated in Singapore and Australia, and consists of a 3-step purification process involving microfiltration, reverse osmosis (RO), and disinfection (Fig. 2).[10] Microfiltration is used to remove particulates and macromolecules from raw water by using membranes with pores of around 1–100 μm in diameter; RO significantly reduces the total dissolved solids, heavy metals, organic pollutants, viruses, and bacteria; disinfection provides a pathogen-free water environment.

Despite the successful implementation of such systems at a large scale, there are several unsolved challenges. A small subset of contaminants which are present in wastewater effluents passes through the RO membrane and resists disinfection. Besides, RO is an energy-intensive unit operation, removes important minerals from water (*e.g.*, F, K, Na, Ca), and is prone to membrane fouling, which can reduce the membrane flux and lead to frequent membrane replacements.[11] Moreover, under typical conditions, only 70–80% of the water being pumped in a typical RO system will be purified, thus leaving up to *ca.* 20–30% of the effluent from the RO step retained as concentrate and discharged through ocean outfalls or onto the ground.[11] This wastes precious water resources and creates major damage to ecosystems. Finally, such RO plants require expensive and large-scale infrastructure, high capital costs, and engineering expertise, all of which preclude their use in much of the world, particularly in developing countries and sparsely populated areas.[12]

The disinfection step has also major technical challenges, producing carcinogenic and genotoxic by-products, and being ineffective against new forms of protozoa, bacteria, and viruses, independent of the type of disinfectant agent used (Table 2).[4] No solution to these problems exists. Therefore, the development of efficient, reliable, affordable, and sustainable water treatment plants for distributed applications is a need. It has been hypothesized that the next-generation water remediation plant would skip RO, be performed off-grid, have zero liquid discharge, be green and

Table 1 Major emerging contaminants found in 'clean' effluents coming out from wastewater treatment plants. The table points to the fact that current wastewater technologies are no longer suitable to remove emerging contaminants

Group	Class	Function	Major contaminants (individual average concentration)[a]	Overall average concentration[a]
Drugs and pharmaceuticals	Analgesics	Help relieve pain	Tramadol (218.4), diclofenac (43.3), codeine (20.9), naproxen (8.2), ibuprofen (7.0), paracetamol (<0.1), ketoprofen (<0.1)	297.8
	Antiarrhythmics	Suppress abnormal rhythms of the heart	Bisoprolol (15.7), flecainide (10.8)	26.5
	Antibiotics or antibacterials	Help the body fight infection	Sulfamethoxazole (231.6), trimethoprim (178.3), ciprofloxacin (82.1), fluconazole (67.5), clindamycin (45.9), tetracycline (0.1)	605.5
	Anticonvulsants or antiepileptics	Treat epileptic and non-epileptic seizures	Carbamazepine (751.9)	751.9
	Antidepressants	Treat depressive disorders	Venlafaxin (97.0), citalopram (21.1), fluoxetine (7.6)	125.7
	Antihistamine	Treat allergies	Fexofenadine (58.8), diphenhydramine (4.9)	63.7
	Antihypertensives	Treat hypertension	Telmisartan (120.1), irbesartan (85.4), bisoprolol (15.7), eprosartan (13.7), diltiazem (6.4)	241.3
	Antipsychotics	Treat schizophrenia, or CNS disorders	Risperidone (17.0), memantin (3.7)	20.7
	Fibrates	Reduce body's cholesterol	Gemfibrozil (4.9)	4.9
	Sedatives	Promote calming effects, *e.g.* sleep	Oxazepam (64.3), haloperidol (0.3)	64.6
Pathogens	Bacteria	Produce bacterial infections	*E. coli* (20), *Salmonella* (18), *Somatic coliphage* (14), *Enterococci* (7)	59
	Viruses	Produce viral infections	*Norovirus* (314), *Rotavirus* (246), *Reovirus* (5), *Enterovirus* (<1)	565

[a] Expressed in nanograms per litre (ng L^{-1}) for drugs and pharmaceuticals, in colony forming units per millilitre (CFU mL^{-1}) for bacteria, and in plaque-forming units per millilitre (PFU mL^{-1}) for viruses. In some cases, reactivation and regrowth of indigenous bacteria and viruses in reclaimed water after disinfection have been observed. Concentration data from the literature.[113–117]

yield fresh and pathogen-free water, without continuous displacement due to pathogen regrowth and fouling.[12] Ideally, it will also recover waste chemicals in a circular manner, to finally close the carbon cycle.

State-of-the-art of integrated photocatalytic solutions for wastewater treatment

Catalytic advanced oxidation processes (AOPs) are promising alternatives to the 3-step purification technique described above.[18] The process uses hydroxyl radicals ($^{\bullet}OH$) to oxidize organic pollutants and harmful pathogens into possibly less toxic and more biodegradable products[19,20] (Fig. 3), following the steps below:

$$\text{photocatalyst} + h\nu \rightarrow e_{CB}^{-} + h_{VB}^{+} \quad \text{(excitation)}$$

$$H_2O + h_{VB}^{+} \rightarrow {}^{\bullet}OH + H^{+} \quad \text{(oxidation of } H_2O\text{)}$$

$$O_{2(ads)} + e_{CB}^{-} \rightarrow O_2^{\bullet-} \quad \text{(reduction of adsorbed } O_2\text{)}$$

$$H^{+} + O_2^{\bullet-} \rightarrow {}^{\bullet}OOH \quad \text{(reaction with } H^{+}\text{)}$$

$$\text{pollutant} + {}^{\bullet}OH + {}^{\bullet}OOH \rightarrow CO_2 + H_2O \quad \text{(oxidation of pollutants)}$$

However, since adsorption is one of the key steps for a good (photo)catalytic performance, pollutants can also be degraded at the catalyst surface by direct oxidation with h_{VB}^{+} or with e_{CB}^{-}:[20]

$$\text{photocatalyst} + h_{VB}^{+} \rightarrow \text{intermediates} \rightarrow CO_2 + H_2O$$

$$\text{photocatalyst} + e_{CB}^{-} \rightarrow \text{intermediates} \rightarrow CO_2 + H_2O$$

Based on these elementary steps, we would expect the formation of the most thermodynamically stable H_2O and CO_2 products, which could be used as platform molecules for

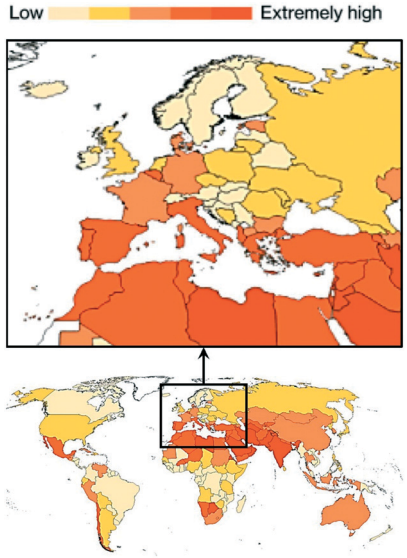

Fig. 1 Countries at risk of water shortage. To prevent that, it is important to shift the paradigm of wastewater management from 'treatment and disposal' to 'recovery, reuse, and recycle', finding new and effective routes to augment water supply systems which are contaminated with pharmaceuticals and waterborne pathogens.

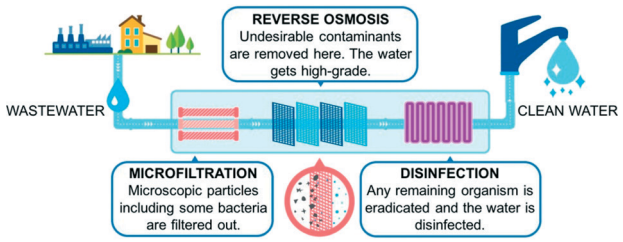

Fig. 2 Today's continuous-flow wastewater purification plant which includes energy-intensive microfiltration, reverse osmosis, and disinfection steps. Such plants are implemented worldwide, and replace less-effective traditional wastewater technologies consisting of two basic steps: filtration and biological treatment.

the downstream synthesis of value-added compounds. In reality, the selective formation of H_2O and CO_2 has been rarely monitored (*vide infra*), and by-products that are even more toxic than the initial substrate are formed, due to the incomplete degratation of the pollutants.[20,21] As a result, toxicity monitoring of the treated water samples has remained an important quality measurement towards water treatment.[22]

Several AOPs have been proposed over the years (*i.e.*, redox agent-based processes based on the traditional or heterogeneous Fenton process, light-driven processes based on semiconductor nanoparticles, and electrochemical-driven processes).[23] In this context, light-driven flow technologies based on the assisted use of photocatalysts are considered sustainable options for wastewater remediation.[24–26]

Nanocrystalline TiO_2 (and in particular TiO_2 Degussa P25) has been the most popular and widely used photomaterial, due to its low cost, characteristic semiconductor bandgap, and ability to form hydroxyl radicals in the presence of water, oxidising pollutants under ambient conditions.[27–29] However, TiO_2 cannot absorb a large fraction (almost 95%) of the solar light, and thus photocatalysts based on TiO_2 doped with metals (*e.g.*, Fe^{3+}, Co^{3+}, and Ag^{+} among others) and non-metals (*e.g.*, C, N, B, F, P, and S) have been developed.[28,29] The dopant serves as an effective electron sink and facilitates charge transfer across the resulting TiO_2 Schottky barrier, giving an optimal bandgap and helping to absorb a higher fraction of visible light. And this potentially results in higher selectivities to H_2O and CO_2. Nevertheless, all doped photocatalysts to date have shown a lower activity compared to the unmodified TiO_2 catalyst, since the band-edge positions in the semiconductor material are not compatible with the electrochemical potential that is necessary to trigger specific redox reactions.[28] In addition, it has been demonstrated that metal species can easily leach from oxides such as TiO_2, which is a serious concern when the dopant is a carcinogenic and genotoxic metal.[28] It is thus unsurprising that the practicality of the TiO_2 doping strategy has been heavily reconsidered in recent years.

As a result, the design of new photocatalysts has not progressed beyond TiO_2 Degussa P25 and, despite the large number of publications dedicated to catalysts with better efficacy, the industrial exploitation of this technology is very limited (Fig. 4).[23]

More recently, researchers have started to explore alternative photocatalysts for the removal of pharmaceuticals and pathogens and the selective recover of chemicals in the form of CO_2, evaluating the use of ZnO, CeO_2, ZrO_2, SnO_2, WO_3, Fe_2O_3, $BiVO_4$, $SrTiO_3$, Ag_3PO_4, CdS, and g-C_3N_4 (see also Table 3).[30] Among those, WO_3 is particularly interesting because it is an n-type semiconductor with a conduction band edge slightly more positive than the H_2/H_2O reduction potential and a valence band edge much more positive than the H_2O/O_2 oxidation potential. WO_3 is thus able to efficiently photooxidize a wide range of organic compounds, such as textile dyes and pharmaceutical pollutants, within the blue region of the visible spectrum. Based on this consideration, Zhao and Miyauchi developed a scalable route to high-purity tungstic acid hydrate nanotubes and nanoporous-walled WO_3 nanotubes.[31] They also found that WO_3 nanotubes loaded with Pt nanoparticles show higher visible-light-driven photocatalytic activity than commercial WO_3. The group of Ye has reported instead Ag_3PO_4 as an active photocatalyst for the photodecomposition of organic compounds.[32] They have achieved a 90% quantum efficiency under visible-light irradiation.[32] The authors also examined the effects of the photocatalyst shapes and facets, preparing single-crystals of Ag_3PO_4 with rhombic dodecahedral shapes displaying (110) facets, and single-crystals of Ag_3PO_4 cubes with (100) facets. The photocatalytic degradation of methyl orange and rhodamine B dyes indicated that the rhombic particles manifested higher photocatalytic activity than the cubic ones under visible-light radiation. Another oxide with a narrow bandgap (2.4 eV), possessing superior visible-light

Table 2 Major continuous disinfection technologies applied today and their limitations[4]

Disinfecting agent	Advantages	Limitations
Chlorine[13]	- Well-established disinfection technology	- Ineffective against protozoa (such as *C. parvum*) and viruses - Formation of by-products (*i.e.*, trihalomethane and haloacetic acid) that have detrimental effects on human health - Taste and odour issues
Monochloroamines[13]	- No by-products - No taste and odour issues	- Ineffective against a variety of helminthes, protozoa, fungi, bacteria, viruses, and prions
Ozone[14]	- Highly-effective disinfectant against micropollutants, including protozoa	- Ineffective against viruses - Formation of by-products (*i.e.*, bromates) that have detrimental effects on human health - Complex, cost- and energy-intensive
Chlorine dioxide[15]	- Well-established disinfection technology	- Ineffective against protozoa (such as *C. parvum*) and viruses - Formation of by-products (*i.e.*, chlorites and chlorates) that have detrimental effects on human health
Hydrogen peroxide and/or peroxone[16]	- None	- Ineffective - No potential for process intensification (*i.e.*, difficulty of preparing highly-concentrated solutions, instability during storage)
UV light[17]	- Highly-effective against micropollutants, including protozoa (such as *C. parvum*)	- Ineffective against viruses

photocatalytic properties is $BiVO_4$. Besides being an n-type semiconductor, this compound is stable, non-toxic, cheap, and can be obtained by numerous methods, such as solid-state reaction, metal–organic decomposition, hydrothermal treatment, and coprecipitation. Zhang, for example, reported $BiVO_4$ nanosheets with a monoclinic structure and preferred (010) surface orientation.[33] There are also promising catalysts based on carbon.[34,35] For example, Li *et al.* prepared activated carbons modified by using concentrated H_2SO_4.[36] This treatment greatly increased the mesoporous volume and the acidic surface oxygen of the material, resulting in greater adsorption of methylene blue and dibenzothiophene than the unmodified carbon. Similarly, graphitic carbon nitride (g-C_3N_4) has attracted attention as a low-cost and visible-light responsive photocatalyst.[37] This material is not only the most stable allotrope of carbon nitride under ambient conditions, but also has tuneable porosity and rich surface properties (presence of basic surface sites) that are intriguing for catalysis.[38] It has been shown that bandgap engineering of g-C_3N_4 to control its light absorption ability (which takes place in the visible range) and redox potential can play an important role in enhancing its photocatalytic performance.[38]

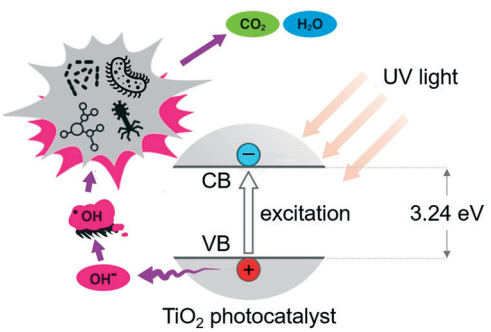

Fig. 3 Mechanism of contaminant removal in a typical continuous-flow advanced oxidation process. The light irradiates the catalyst generating a vacancy at the valence band and forming hydroxyl species. These oxidize pathogens and pharmaceutical contaminants, generating CO_2 (that can be recovered) and H_2O. Nanocrystalline TiO_2 has been the most popular and widely used material investigated in the scientific literature, but the industrial exploitation of this technology has been limited. More recently, researchers have started to evaluate alternative photocatalysts (non-TiO_2-based) for water purification in flow.

Theoretical calculations based on density functional theory, molecular dynamics, and kinetic Monte Carlo are complementing the search for non-TiO_2 catalysts. In particular, calculations have shown that some of these materials (such as Ag_3PO_4 and ZnO) are not considered ideal due to concerns with the leaching and photocorrosion of the nanomaterials (in the form of metal or ions) into ecosystems.[30] However, more work is required to tune the material nanostructure.

As shown in Tables 4 and 5, only a few (*i.e.*, five) studies published in the last decade have analyzed the selectivity to the desired CO_2 product. Often, researchers have focused instead on the pollutant degradation rate, without attentioning the catalytic and selective formation of less toxic and more biodegradable products. As a result, by-products that are more toxic than the initial substrate have frequently been formed,[31,36] and independently of the materials used, their structures have remained unknown. Such knowledge gap is a major deficit for a society that intends to become 'circular': when selectively obtained, CO_2 can become a platform molecule to make plastics, fertilizers, and more. One question at least arises: what can we learn from these five studies? It is in general difficult to compare these works due to differences among preparation methods and test conditions. Nevertheless, some guidelines can be placed and these can guide the rational design of ultraselective catalytic materials and processes for photo-oxidation. For these reasons, the following sections will analyse in a critical manner those strategies.

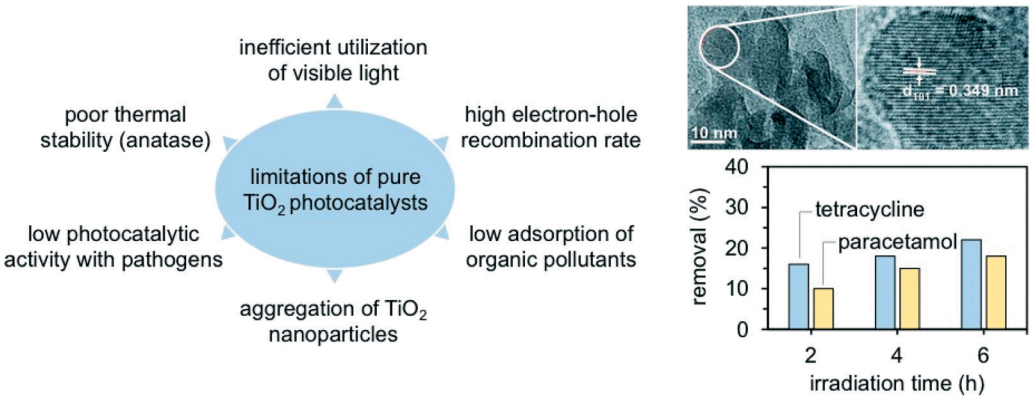

Fig. 4 Limitations in the use of TiO_2 Degussa P25 for the removal of emerging pharmaceutical pollutants in flow mode. Titania cannot absorb a large fraction of the solar spectrum, resulting in a low photocatalytic activity. This is exemplified on the right, where TiO_2 particles with well-defined surface properties show a low efficiency (10–20% conversion) in the removal of tetracycline and paracetamol, independent of the chosen irradiation time.

Table 3 Crystallographic and electronic properties of TiO_2 and non-TiO_2-based materials. Most of these catalysts have suboptimal properties, thus requiring structural and compositional tuning *via* materials engineering

Photocatalyst	Crystal system	E_{gap} [a] (eV)	λ_{abs} [b] (nm)	E_{CB} [c] (V *vs.* NHE[e])	E_{VB} [d] (V *vs.* NHE)	Ref.
TiO_2 rutile	Tetragonal	*ca.* 3.0	388	+0.04	+3.04	39
TiO_2 anatase	Tetragonal	*ca.* 3.2	388	−0.16	+3.04	39
ZnO	Hexagonal	*ca.* 3.2	388	+0.21	+3.41	40, 41
CeO_2	Cubic	*ca.* 3.2	388	−0.07	+3.13	42
ZrO_2	Monoclinic	*ca.* 5.0	248	−0.69	+4.31	41, 43
SnO_2	Tetragonal	*ca.* 3.5	354	+0.25	+3.75	41, 44
WO_3	Monoclinic	*ca.* 2.7	443	+0.77	+3.47	41, 45
Fe_2O_3	Trigonal	*ca.* 2.2	564	+0.79	+2.99	41, 46
$BiVO_4$	Monoclinic	*ca.* 2.4	517	+0.49	+2.89	47, 48
$SrTiO_3$	Cubic	*ca.* 3.4	365	−0.75	+2.65	41, 49
Ag_3PO_4	Cubic	*ca.* 2.4	517	+0.50	+2.90	50
CdS	Hexagonal	*ca.* 2.4	517	−0.40	+2.00	41, 51
g-C_3N_4	2D	*ca.* 2.7	459	−0.90	+1.80	52

[a] Energy of the band gap. [b] Wavelength of the incident light absorption edge. [c] Energy level of the conduction band minimum. [d] E_{VB} is the energy level of the valence band maximum. [e] NHE is the normal hydrogen electrode potential.

Catalyst design strategies

From a catalyst design viewpoint, the materials mentioned in the previous section can be classified into 'metal oxides', 'metal sulphides', 'metal phosphates', and 'metal-free materials'. Table 3 summarizes their physical–chemical properties, and Fig. 5a shows their most common crystal structure.

Different methods exist to prepare these materials. These can be 'gas-phase methods' and 'liquid-phase methods'. Gas-phase methods, such as physical vapor deposition (PVD), chemical vapor deposition (CVD), atomic layer deposition (ALD), and sputtering, offer a number of synthetic advantages, including atomic-level mixing of the different phases, precise control of the stoichiometry, tuneable grain size and morphology, and physicochemical homogeneity.[53] These routes require, on the other hand, expensive catalyst preparation infrastructures and machineries.[53] Liquid-phase methods, such as precipitation, impregnation, sol–gel, ion exchange, deposition–precipitation, microwave synthesis, or hydrothermal treatment, offer instead simple and inexpensive synthetic processes and flexibility over the control of particle size, exposed facets, and single-crystal grains.[53]

There are, however, a number of emerging techniques which are taking hold in labs around the world: these include mechanochemistry,[54] electrospinning,[55] and electrochemical methods.[56] Ball milling is the most common mechanochemical method because it is simple and suitable for large throughputs, although potential abrasion of the mill may result in the introduction of impurities,[57] which is very critical for photocatalytic applications. Electrospinning and electrochemical methods are also commonly applied for the production of ultrafine nanoparticles with hierarchical porosity and well-defined morphology.

The synthetic method is typically chosen based on the properties which are required in the material. A key aspect in the selection of the design strategy remains the ability to manipulate the catalyst properties with the route selected. This aspect is critical, since the pristine materials in Table 3

Table 4 TiO_2-based photocatalysts employed for the removal of emerging pharmaceutical contaminants. In the past decade, most of the research work has focused on maximizing the contaminant conversion. However, it is well-known that, in the process, toxic by-products can be formed. It is envisioned that next-generation processes will focus on rational catalyst, reactor, and process design to maximize the selectivity to the thermodynamically stable CO_2 and H_2O products. The table also shows the knowledge gap in unlocking selectivity patterns on the different catalysts

Class	Contaminant	Photocatalyst[a]	Reaction source	Influence pH or ions	Contaminant concentration (ppm)	Removal (%)	Selectivity CO_2 (%)	Ref.
Analgesics	Paracetamol	$BaTiO_3/TiO_2$	UV-vis, 200–800 nm, 500 W	Yes	10	83	—[b]	118
		$WO_3/TiO_2/SiO_2$	UV-vis, 200–800 nm, 500 W	Yes	10	88	—	119
		C-Doped TiO_2	Vis, 440–490 nm, 5 W	No	15	94	—	120
		TiO_2/montmorillonite	UV with ozonation, <400 nm, 8 W	No	5	50	—	121
	Diclofenac	C-Doped TiO_2	Vis, >400 nm, 150 W	Yes	0.05	100	—	122
		C-Doped TiO_2/zeolite	UV-vis (solar light), 300–400 nm with 65 W m^{-2}, and 400–570 nm with 1844 W m^{-2}	Yes	0.1	95	—	123
		TiO_2	UV-vis (solar light), >300 nm, sunny days between July and September	Yes	250	100	—	124
	Ibuprofen	g-$C_3N_4/TiO_2/Fe_2O_3@SiO_2$	Vis, >400 nm, 64 W	Yes	2	98	78	125
		GO/TiO_2	High pressure UV, 160 W	No	5	81	—	126
		GO/TiO_2	Low pressure UV, 39 W	No	5	41	—	126
		GO/TiO_2	Vis, >400 nm, 40 W	No	5	18	—	126
		TiO_2	UV, <330 nm, 40 W	No	213	100	—	127
		TiO_2	UV-vis, 200–800 nm, 60 W	Yes	10	80	—	128
	Ketoprofen	Bi_2S_3/TiO_2	UV, <365 nm, 200 W	Yes	15	80	—	129
		TiO_2	UV, 254–366 nm	Yes	3	16	—	130
		TiO_2–graphene	Vis, 785 nm, 1 mW	No	20	96	—	131
		TiO_2	UV-vis (solar light), >300 nm, 500 W	No	6.8×10^{-4}	33	—	132
	Codeine	TiO_2	UV, 250–400 nm, 500 W m^{-2}	No	10	100	—	133
	Tramadol	TiO_2	UV, 350 nm, 500 W m^{-2}	No	10	94	—	134
	Naproxen	TiO_2	UV-vis (solar light), >300 nm, sunny days between July and September	Yes	250	96	—	124
Antibiotics	Ciprofloxacin	Mesoporous carbon-TiO_2	UV, 254 nm, 14 W	No	15	100	—	135
		TiO_2/montmorillonite	UV with ozonation, <400 nm, 8 W	No	5	81	—	121
		Mesoporous TiO_2	UV-vis (solar light), >300 nm, 500 W	No	160	96	—	136
	Tetracycline	$FeNi_3@SiO_2@TiO_2$	UV, 254 nm, 18 W	No	10	100	—	137
		CNT/TiO_2	UV, 240 nm, 12 W	No	10	100	92	138
	Trimethoprim	TiO_2	UV, 254 nm, 30 W m^{-2}	No	14	19	—	133
		Ag or Au/TiO_2	UV, 254 nm, 30 W m^{-2}	Yes	40	76	—	139
	Clindamycin	TiO_2	UV-vis, 200–450 nm	No	2	100	—	140
	Sulfamethoxazole	TiO_2	UV, <310 nm, 1000 W	No	100	82	—	141
		TiO_2/biochar	UV, 254 nm, 15 W	No	10	74	—	142
		TiO_2/perlite	UV-vis, 250–450 nm, 8 W	No	100	89	—	143
		Mpg-C_3N_4/TiO_2	UV, 270 nm, 300 W	No	10	68	—	144
		$CoFe_2O_4/TiO_2$	UV, 350 nm	Yes	25	55	—	145
Anticonvulsants or antiepileptics	Carbamazepine	C-Doped TiO_2	Vis, >400 nm, 150 W	No	0.05	100	—	122
		C-Doped TiO_2/zeolite	UV-vis (solar light), 300–400 nm with 65 W m^{-2}, and 400–570 nm with 1844 W m^{-2}	Yes	0.1	95	—	123
Antidepressants	Fluoxetine	TiO_2 nanowire	UV-vis, 200–800 nm, 100 W	No	1.0×10^{-4}	100	—	146
	Venlafaxin	TiO_2 nanowire	UV-vis, 200–800 nm, 100 W	No	1.0×10^{-4}	100	—	146
Antipsychotics	Risperidone	GO–TiO_2	UV-vis, 290–430 nm, 1500 W	No	10	78	—	147
		TiO_2	UV-vis, 290–430 nm, 1500 W	No	10	73	—	147

Table 4 *(continued)*

Class	Contaminant	Photocatalyst[a]	Reaction source	Influence pH or ions	Contaminant concentration (ppm)	Removal (%)	Selectivity CO_2 (%)	Ref.
Fibrates	Gemfibrozil	TiO_2/carbon dots	UV, <290 nm, 350 W	No	2	84	—	148
		TiO_2	UV, 220 nm, 125 W	No	10	100	—	149
		TiO_2	UV, 254 nm, 125 W	No	2.2×10^{-4}	88	—	132

[a] CNT: carbon nanotubes; GO: graphene oxide; Mpg: mesoporous graphitic. [b] Not investigated and/or not reported.

exhibit suboptimal photocatalytic properties. In fact, the energy levels of the conduction band minimum (E_{CB}) and valence band maximum (E_{VB}) point to the reducing ability of their photogenerated electrons (large negative E_{CB}) and the oxidizing ability of their photogenerated holes (large positive E_{VB}). In order to produce stable radicals, it is expected that E_{CB} would be more negative than $O_2/O_2^{\bullet-}$, while E_{VB} would be more positive than $H_2O/^{\bullet}OH$. In an attempt to enhance these characteristics, which would lead to the desired CO_2 and H_2O products, the pristine catalysts are thus modified *via* morphology tuning, elemental doping, and composite formation (Fig. 5b). A combination of experimental and theoretical tools can be applied to corroborate the properties obtained at different length scales and rationally optimise the materials further (Fig. 5c).

Morphology and vacancy engineering

This approach can effectively increase the selectivity to the desired CO_2 and H_2O products. It is well known that, given a certain crystal, the facet at the surface is key since it is there that catalysis takes place. This facet offers exposed atoms with a defined coordination number, providing a knob for tuning the catalytic activity. The tuning of the type of exposed facet is practically done by preparing nanomaterials with different morphologies (*e.g.*, nanocubes, nanooctahedra, nanorods), using liquid-phase methods such as sol–gel, hydrothermal treatment, and colloidal synthesis.[58–62] There are many examples in the literature depicting the use of nanoparticles with variable morphologies to enhance the catalytic turnover.[63–66] Uniform Au nanoparticles with different shapes (cubes, rods and spheres) were prepared, for example, to evaluate the influence of the catalyst morphology on the degradation of dyes.[67] In particular, gold nanospheres and nanorods were purchased from Sigma-Aldrich; nanocubes were instead synthesized by adding freshly prepared $NaBH_4$ into a colloidal gold solution, made by mixing $HAuCl_4^-$ and cetyltrimethylammonium chloride. The mixture was kept under stirring for a few hours in order to have particle growth. Finally, ascorbic acid was added to the yellow-coloured mixture under gentle stirring, leading to a colourless liquid containing concave Au nanocubes. Evaluated in catalysis, the degradation efficiencies and CO_2 selectivity were in the order nanocubes > nanorods > nanospheres.[67] This result was in line with previous work showing similar structure–performance relationships of ceria in oxidation reactions.[58] In fact, the (100) surface, predominantly exposed in nanocubes, is optimal for oxidation. This result can be attributed to the different oxygen vacancy chemistry on these facets,[68,69] which is more prone on the (100) surface and less probable on the (111) facet. At these vacant sites, the catalyst can bind reactants and intermediates. Defects located at the surface (such as anion and cation oxygen vacancies) can also influence the band structure of the photocatalyst to achieve optimal light harvesting and energy transfer.[61,62]

Table 5 Examples of novel non-TiO_2-based photocatalysts for the degradation of pharmaceutical pollutants

Class	Contaminant	Photocatalyst	Reaction source	Influence pH or ions	Contaminant concentration (ppm)	Removal (%)	Selectivity CO_2 (%)	Ref.
Analgesics	Paracetamol	ZnO/sepiolite	UV, <200 nm, 450 W m^{-2}	No	10	85	—[a]	150
		ZnO/Fe_2O_3–sepiolite	UV, <200 nm, 450 W m^{-2}	No	10	55	—	150
		ZnO/SiO_2–sepiolite	UV, <200 nm, 450 W m^{-2}	No	10	20	—	150
		ZnO	UV, 315–400 nm, 18 W	Yes	15	14	—	151
		$ZnO–Fe_2O_3$/GO	UV-vis (solar light), >300 nm, 500 W	Yes	5	95	72	152
	Diclofenac	g-$C_3N_4/BiVO_4$	Vis, >420 nm	No	10	30	—	153
		ZnO	UV, <300 nm, 150 W	No	1	68	—	154
		Co_3O_4/g-C_3N_4	Vis, >420 nm, 300 W	No	10	20	—	155
	Ibuprofen	$ZnO–Fe_3O_4$	UV-vis (solar light), >300 nm, 500 W	Yes	250	96	—	156
		ZnO/sepiolite	UV, <320 nm, 450 W m^{-2}	No	10	100	—	150
		ZnO/Fe_2O_3–sepiolite	UV, <320 nm, 450 W m^{-2}	Yes	10	95	—	150
		ZnO/SiO_2–sepiolite	UV, <320 nm, 450 W m^{-2}	No	10	80	—	150
		ZnO	UV-vis, 200–700 nm, 60 W	No	5	59	—	157
		ZnO	UV, <300 nm, 150 W	No	1	60	—	154
	Ketoprofen	Ag–BiOBr/GO	Vis, 425–496 nm, 300 W	No	1000	100	—	158
	Naproxen	ZnO/montmorillonite	Ultrasound, 650 W, 60 kHz	No	10	73	—	159
Antibiotics	Ciprofloxacin	GO	UV, 285 nm	No	40	98	87	160
	Tetracycline	$AgInS_2/SnIn_4S_8$	Vis, >420 nm, 300 W	Yes	10	77	78	161
		$Ag/AgIn_5S_8$	UV, 254 nm, 9 W	No	10	95	—	162
	Clindamycin	ZnO	UV, 366 nm, 50 W	No	25	78	—	163
Anticonvulsants or antiepileptics	Carbamazepine	BiOCl	Vis, >420 nm, 350 W	No	2.5	70	—	164
Antihistamine	Diphenhydramine	ZnO/Fe_2O_3/zeolite	UV, 254 nm, 6 W	Yes	100	100	—	165
Antihypertensives	Eprosartan	ZnO	UV, 365 nm, 8 W	No	0.56×10^{-6}	95	—	166
	Irbesartan	ZnO	UV, 365 nm, 8 W	Yes	1.5×10^{-6}	95	—	166

[a] Not investigated and/or not reported.

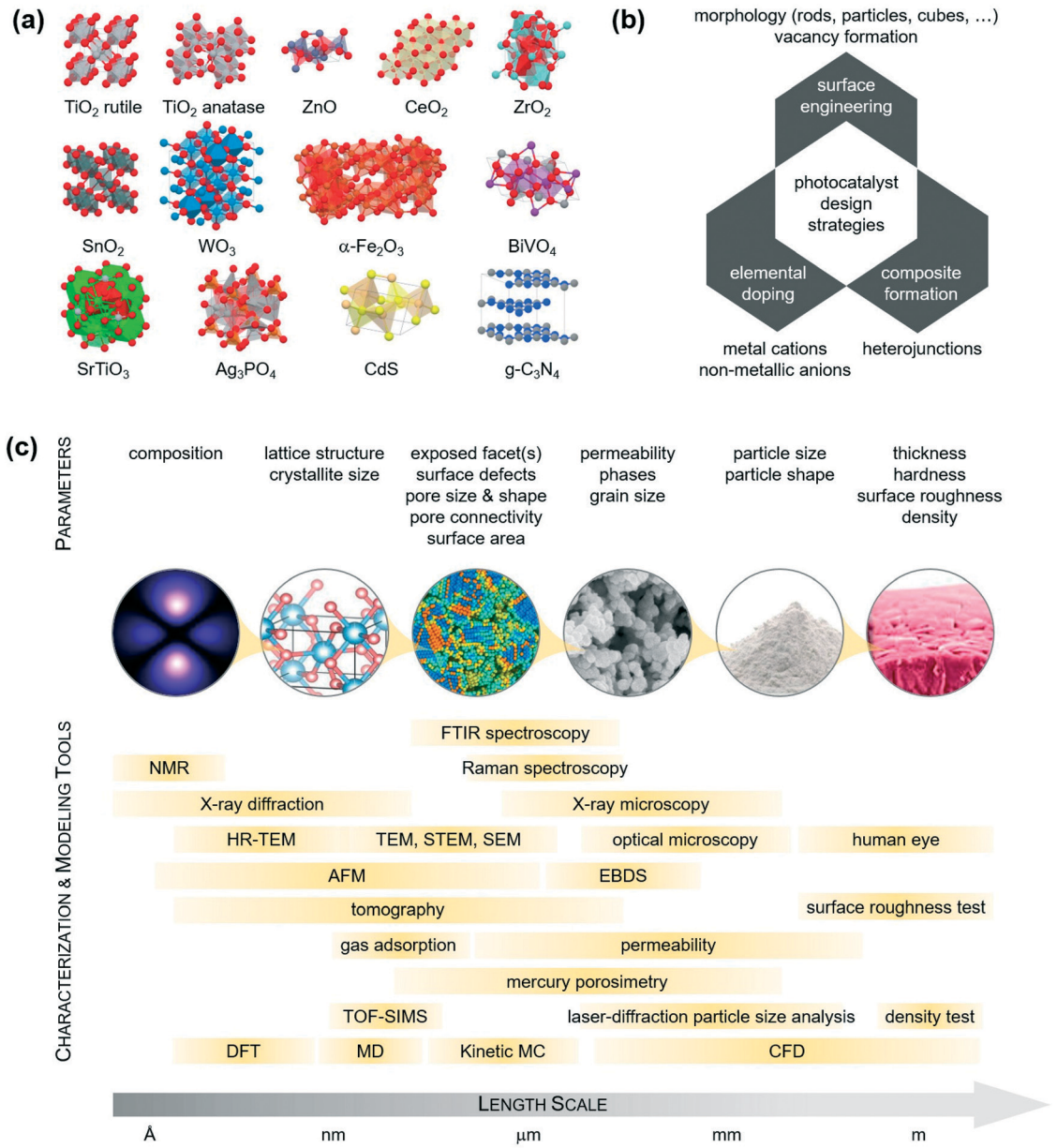

Fig. 5 Crystallographic structures of commonly used photocatalytic materials for continuous-flow wastewater remediation (a), design and synthesis strategies (b), and set of important characterization and computational methods to assess structural, physical, and chemical properties at different length scales and rationally design the next generation catalytic processes (c).

Elemental doping

Doping is another effective strategy to develop excellent photocatalytic materials for wastewater remediation and enhance, at the same time, the material band structure and the product selectivity. Doped photocatalysts are typically prepared *via* sol–gel, CVD, or ALD.[70] The most used dopants in water catalysis are transition metal ions, such as Fe^{3+}, Co^{3+}, Ag^{+}, Cu^{2+}, Mo^{5+}, Cr^{3+}, and V^{4+}.[71–74] The introduction of these ions leads in most cases to a band state near the CB or VB edge of a semiconductor, effectively shifting the adsorption wavelength from UV to visible light. The approach, however, suffers from several drawbacks, such as thermal instability and significant increase in the carrier recombination in which the metal acts as an electron trap and ultimately reduces the photocatalytic performance. For this reason, doping with non-metallic anions (*e.g.*, C, N, B, F, P, and S) has been considered as a better alternative to regulate the intrinsic electronic structure of the pristine materials.[75,76] In particular, catalytic tests have shown that N is the most effective dopant for reaching visible-light photocatalysis. Salah *et al.*, for example, obtained a series of ZnO nanoparticles doped with substitutional and interstitial N species.[76] In this work, the pure ZnO film was evaporated at high temperature and then deposited on a glass surface with simultaneous addition of N_2 gas. The level of N-doping

was tuned by adjusting the flow rates of N_2 during the deposition process. The materials possessed an improved response to visible light and significantly enhanced the degradation of antibiotics under the drive of natural sunlight, reaching an excellent 86% selectivity to CO_2 and H_2O (Fig. 6).[76] Similarly, for the removal of ibuprofen, B-doped TiO_2 showed an excellent photocatalytic performance compared to pristine TiO_2 (removal rates of 85% and 25% for B-doped TiO_2 and pure TiO_2, respectively), due to the enhanced crystallinity and electronic properties of TiO_2.[77,78] Interestingly, the authors explored an alternative preparation route where B-doped TiO_2 synthesis was carried out following a modified solvothermal procedure. Here, tetrabutyl titanate, boron, and boric acid were mixed in ethanol; the solution was hence added to an acidic PEG-600 mixture. The sol was first stirred and then aged for several days, thus undergoing high-temperature hydrothermal treatment in a Teflon-lined stainless-steel autoclave.

Composite formation

Heterostructures, which are often prepared *via* sol–gel, electrospinning, microwave synthesis, or hydrothermal routes, offer opportunities to improve the activity and product selectivity by tuning band structures and promoting carrier transfer. Wang *et al.*, for example, fabricated $SnFe_2O_4$/$ZnFe_2O_4$ nanoheterojunctions following a one-pot hydrothermal strategy.[79] The structures exhibited under visible light conditions excellent photocatalytic degradation

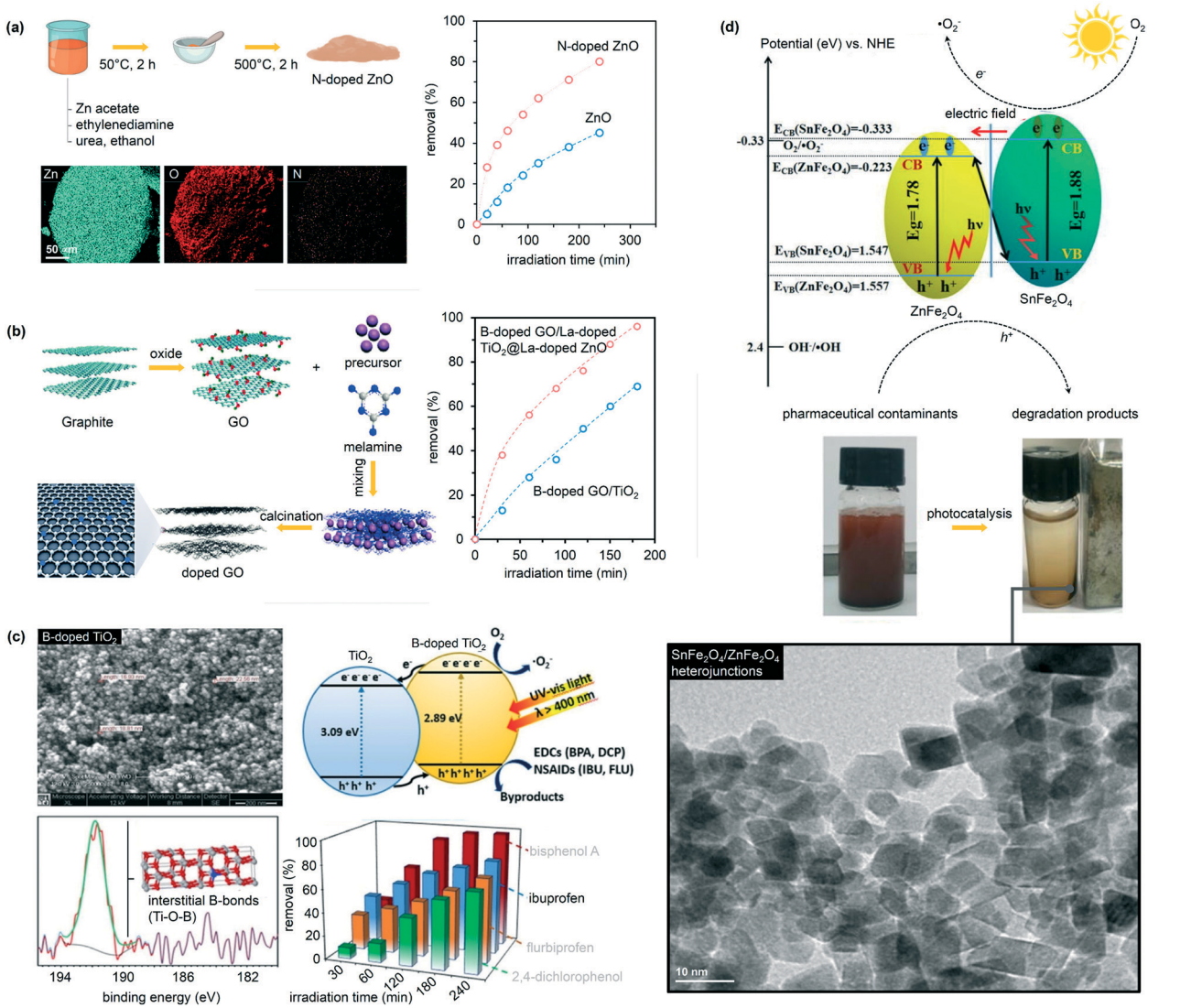

Fig. 6 Selection from the literature showing the influence of catalyst doping and heterojunction formation in water purification. The figure features the role of N doping on ZnO catalysts in the removal of 2,4-dichlorophenoxyacetic acid (a); the synthesis of B-doped graphite oxide (GO) particles and their use for the removal of diclofenac (b), the role of B doping on TiO_2 for the removal, among other pollutants, of ibuprofen (c), and the role of magnetic $SnFe_2O_4$/$ZnFe_2O_4$ nanoheterojunctions in eliminating tetracycline. Adapted from ref. 76–79. Copyright Royal Society of Chemistry (a and b) and Elsevier (c and d).

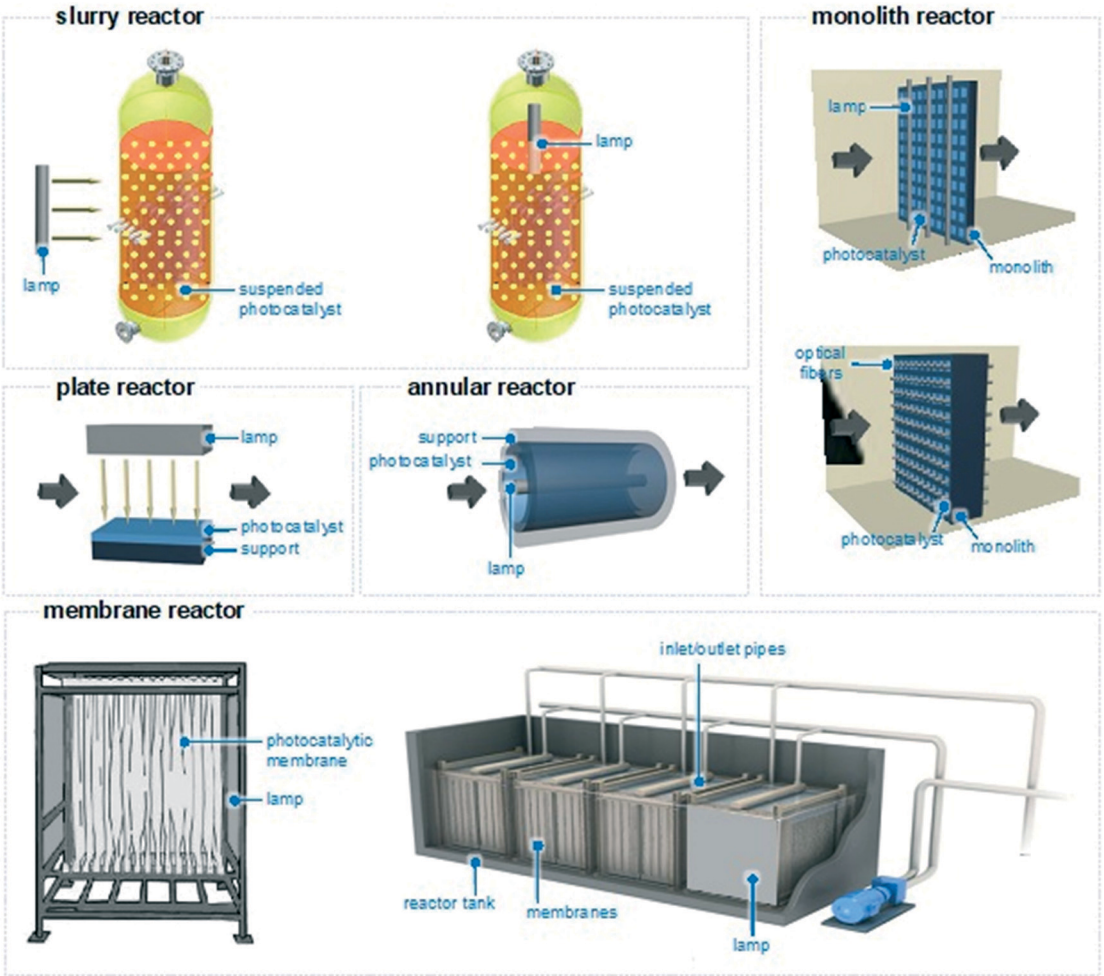

Fig. 7 Selection of different reactor configurations for the removal of pharmaceutical pollutants from water. More complex reactor geometries are possible but are not displayed here for the sake of conciseness.

of tetracycline, demonstrating 93% removal and a selectivity to CO_2 and H_2O of 78% (Fig. 6). Toxicology studies confirmed as well the nontoxicity of $SnFe_2O_4/ZnFe_2O_4$, proving that the environmentally friendly heterojunction could be a promising photocatalyst for wastewater treatment. Similarly, heterojunctions made of Ag/C-dots and g-C_3N_4 and prepared by thermopolymerization showed 88% removal of naproxen and 83% H_2O selectivity under visible light conditions and in only 24 min of reaction time.[80]

Lessons learned and future steps

This section has revealed that advances in the engineering of functional nanomaterials can offer new opportunities in designing a family of continuous water treatment processes to remove emerging contaminants, while ensuring formation of biodegradable products, such as the thermodynamically stable CO_2 and H_2O. Nevertheless, while most of these materials have shown promises at a lab scale, their future industrial implementation faces today a variety of challenges and technical hurdles. One important aspect that requires consideration is whether the photocatalyst is effectively activated by light, and the type of light (*i.e.*, UV, visible light, *etc.*) which is required. The retention and reuse of nanocatalysts is another key aspect of sustainability in an age of resource scarcity, with consequences on process cost and public health. Catalysts, even in heterogenized forms, show in fact biotoxicity and slow environmental degradation.[81] The large-scale adoption of these technologies strongly depends on the potential risks involved. Today, little is known about the photocorrosion of the catalysts in the reactors. It is often assumed that catalyst leaching can be minimized by immobilizing the nanomaterials on a solid support. Unfortunately, leaching phenomena are largely dependent on the technique used to immobilize the nanomaterials.[82] Generally, nanomaterials coated on solid surfaces are likely to be released in a relatively fast and complete manner, while nanomaterials embedded in a solid matrix will have minimum release until they are disposed of.[82] A better understanding of these potential hazards could lead to finally fill some of the knowledge gaps on materials development.

Reactor design strategies

The reactor configurations used to remove water pollutants are mainly categorized into four types: slurry reactors, plate and annular reactors, honeycomb monoliths, and membrane catalytic reactors (Fig. 7). To remove the pollutants and enhance the selectivity to biodegradable products, there is no optimal geometry; all systems have in fact advantages and disadvantages. Therefore, for the design and construction of a reactor, the type of catalyst, the irradiation source (natural or artificial), the light source position (immersed or external), and the desired kinetics are all parameters to be assessed to make a reactor selection.[83] Technical implementation challenges (for example related to the geographical location where the reactor is going to be installed) and economic considerations are also important factors. Therefore, the reactor chosen depends not only on the reaction under investigation but also on considerations made by the engineers investigating water remediation.

In a slurry reactor,[84,85] the photocatalyst is mixed with the contaminated water to form a heterogeneous suspension kept under magnetic stirring. The lamp is placed internally or externally and irradiates the catalytic particles. Assuming that the light is at the right wavelength where pharmaceuticals absorb light, these will absorb photons from the artificial light source and then react at the solid–liquid interface. The reaction tank is typically made of pyrex or quartz and a water jacket may surround the tank to keep the temperature of the reaction process uniform. These reactors ensure low pressure drop, high convective mass transfer rate, and higher photon utilization, leading to moderate to high selectivity to CO_2 and H_2O. Yet, separation and removal of the photocatalytic phase is onerous and involves downstream separation methods (*i.e.*, filtration) which could be hazardous when handling pyrophoric catalysts. In such reactors, the kinetics of photodegradation follows typically the Langmuir–Hinshelwood mechanism.[86] The reactor design can alleviate some of the problems of slurry reactors and increase their efficiency. For example, rotating photocatalytic contactors have been shown to effectively degrade water recalcitrant pollutants and the rate of degradation increased with the rotation speed.[87,88]

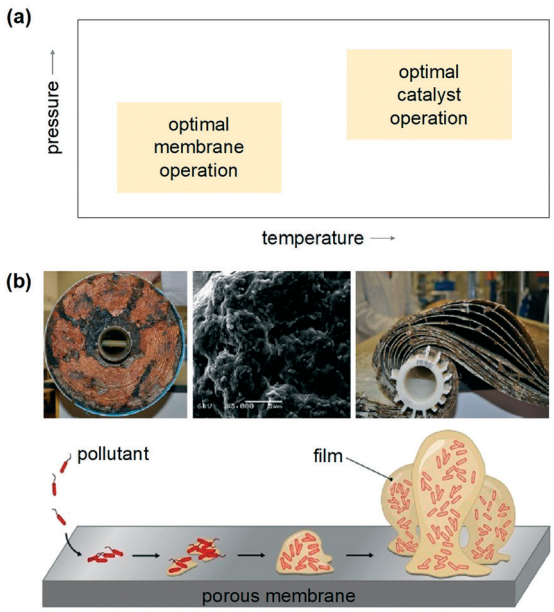

Fig. 8 Technical and scientific issues with membrane reactors. The figure in particular highlights the gap in operating windows between the catalyst and the membrane (a) and the extent and causes of membrane fouling (b).

Plate and annular continuous reactors are alternative configurations for selective water treatment.[89] In these continuous reactors, the photocatalyst is coated onto a support (that can be planar or cylindrical) and the lamp irradiates perpendicularly the catalyst, on top of the plate or at the centre of the cylinder.[90–92] These reactors ensure simple geometries and low pressure drops, but often provide less selectivity towards CO_2 and H_2O and more toxic by-product formation. This is due to the low convective mass transfer rate associated with the limited area available for the reaction, which remains one of the major disadvantages in this type of reactor.[92] Complex geometries featuring multi-plate and multi-annular reactors have been also developed to ensure greater convective mass utilization, although they might provide higher pressure drops.[93,94]

In monolith reactors, the photocatalyst is placed (for example by dip-coating) on the monolith and the light is close to that.[95,96] This geometry ensures high mechanical strength, high reaction area, and good transport phenomena, leading to higher product selectivities. Yet, there might be issues with the low photon utilization rate when the monolith is thick. The lamp may be substituted with optical fibres to ensure higher photon utilization, but paying the price of poor heat dissipation.

Finally, due to their separation efficiencies, relatively low costs, small footprint, and easy operation, catalytic membrane reactors can act as a physical filter for suspended species and, at the same time, bind pathogens and organic impurities and photocatalytically oxidize them to inert CO_2 and H_2O.[97–99] The membranes often feature photocatalytic composites supported on polymeric and metallic nanoporous materials that form the skeleton of the membrane. The reaction takes place at the surface of the membrane, where the catalyst is present, or within its pores. Light irradiation can be in the form of lamps or optical fibres placed closely to the catalytically active sites. In terms of reactor design, the catalyst loading, its mechanical resistance and morphology, and the material permeability are all important factors to be considered and optimized to obtain excellent photocatalytic performances. Overall, membranes can ensure a high level of automation and a modular configuration, enabling flexible design and less land and energy usage.[99] However, various technical issues might be encountered, such as membrane structure deterioration, low photocatalytic activity, loss of the deposited catalytic layer over time, and membrane fouling (*vide infra*).

Lessons learned and future steps

The design of a better, low-cost, and highly-efficient photoreactor capable of absorbing the radiation and promoting reactions with minimal photonic loss is a strategic requirement. Despite extensive research efforts, batch-type slurry photocatalytic reactors remain the preferred configurations at scale,[100] owing to their high total surface area of photocatalyst per unit volume and ease of photocatalyst reactivation. These reactors, however, only provide moderate product selectivities.[76]

In the quest for continuous and more selective operations, it has been proposed that the most important factors for an optimal reactor configuration remain the total irradiated surface area of catalyst per unit volume and the light distribution within the reactor.[101] To achieve light uniformity, a correct position of the light source is essential to ensure maximal and symmetrical light transmission and distribution. Plate and annular continuous reactors have been explored in the past, but they tend to increase the production of unwanted by-products, due to their low convective mass transfer rate given by the limited area available for the reaction.[92] Monolithic reactors and, in particular, catalytic membrane reactors have gained momentum in recent years as they offer the possibility of solving the downstream separation issue of photocatalyst particles, while reaching excellent CO_2 selectivities.[102,103] Yet, a major challenge with the use of membranes is the inherent trade-off between the membrane and catalyst properties (Fig. 8).[103] Combining membranes and catalysts in a closed architecture requires operating both under the same conditions. However, these operating windows do not always overlap and novel materials are required to reduce the operating and investment cost for the process.[103] Going from a lab-scale to a pilot scale sets increasingly higher demands on the lifetime of both catalysts and membranes. Also in this case, for most types of membranes, achieving a commercial life-time target (>10 000 hours) is still far from reality, in particular in 'real' industrial mixtures.[2] Membrane fouling is a major issue for operation and adds to the energy consumption and the complexity of the process operation, reducing the lifetime of membranes and catalytic modules.[2,3,103] As a result, further pilot plant investigations with different reactor configurations are needed to ensure that the photocatalytic water technology is well established and presents vast technoeconomic data for any life cycle analysis study.

A quest for standardised operational parameters and process design conditions

Literature studies have shown that the contaminant concentration, water pH, presence of ions in water, and co-irradiation with ultrasound can have a major effect in improving the performance of the materials and reactors selected.

Contaminant concentration

The concentration of contaminants is a critical element that affects the efficiency and kinetics of contaminant removal. It also affects the design of an optimal photocatalyst. Generally, at low concentrations of contaminants, there are sufficient amounts of $^{\bullet}OH$ radicals and holes for the reaction.[104] As the concentration of contaminants increases, more reactant molecules are adsorbed on the catalyst surface, reducing the generation of $^{\bullet}OH$ due to the presence of fewer active sites.[104] At very high contaminant concentrations, the photons are absorbed by the contaminants even before they can reach the catalyst surface.[104] This decreases the overall photocatalytic efficiency and may also cause the deactivation of the catalyst due to fouling, which is more prominent for catalysts with larger crystals.[105] These studies highlight the importance of conducting catalytic tests under water-relevant experimental conditions, and at a concentration of contaminants which is similar to that found in wastewater. As shown in Tables 4 and 5, very few studies have taken so far this critical parameter under consideration. A guideline for future investigation is to conduct all catalytic tests at the pollutant concentrations indicated in Table 1.

Water pH

The pH of the aqueous phase is an important factor in photochemical reactions since it controls the size of the generated aggregates and the surface charge properties of the photocatalyst.[106] This is particularly relevant for metal oxides that have an amphoteric behaviour, such as ZnO and SnO_2. These catalysts can be positively or negatively charged, depending on the pH of the solution. For example, the point of zero charge of ZnO is 9.3.[107] Thus, above this pH, the surface of ZnO is negatively charged and features adsorbed OH^- ions. These may increase the production of $^{\bullet}OH$ radicals, leading to holes (h^+) and hydroxyl radicals that act as oxidation agents. On the other hand, at lower pH values, photogenerated holes are the sole oxidizing species.

The electric charge properties of the contaminants are also important. The contaminant, in fact, is in a molecular form when the pH is less than its pK_a, while at pH > pK_a, the compound loses a proton and becomes negatively charged.[108] Obviously, when the charges of the catalyst and contaminants are the same, the removal efficiency decreases due to the repulsion forces between the catalyst surface and the substrate.

Presence of ions

The effect of the water matrix is very important, since carbonates, nitrates, chlorine, sulphates, and phosphate ions are commonly found in water and are present in the effluent of several treatment plants. These act as a filter,[109] absorbing light energy and reacting with $^{\bullet}OH$ radicals, ultimately decreasing the rate of photocatalytic degradation. For carbonates, we have:

$$CO_3^{2-} + {}^{\bullet}OH \rightarrow OH^- + CO_3^{-}$$

$$HCO_3^- + {}^{\bullet}OH \rightarrow H_2O + CO_3^{\bullet-}$$

Another important aspect is the preferential adsorption of the cationic or anionic molecules (carbonates, nitrates, chlorine, sulphates, and phosphates) on the catalyst surface,[109] leading to catalyst deactivation. A lot has been done to study the catalytic removal of ions in natural water (not the water prepared in the laboratory by adding a salt to distilled water), using a continuous stirred tank reactor. Corma *et al.*, for example, studied the performance of Cu–Pd or Sn–Pd supported on alumina catalysts in removing nitrates.[87] They analysed and optimized the Pd-metal ratio and the reaction conditions, showing that the activity of the catalysts in the water nitrate reduction depends on the type of water used.[87] In water with a high conductivity and hardness, the best results are obtained when using a Pd : Sn catalyst with a Pd : Sn ratio of 2. The results obtained also showed that the catalyst deactivation in water with a high conductivity and hardness was probably related to the fouling and poisoning of the palladium centres due to precipitation of calcium salts on the catalyst surface and the presence of sulphur compounds in water.

Ultrasound irradiation

In recent years, ultrasound irradiation has emerged as an enabling technology to be employed together with light irradiation.[110] In this case, the formation, growth, and implosive collapse of bubbles increase the catalyst surface activity and enhance transport phenomena,[111] producing free radicals as shown below:

$$H_2O + \text{ultrasound} \rightarrow {}^{\bullet}OH + {}^{\bullet}H$$

$$O_2 + \text{ultrasound} \rightarrow 2{}^{\bullet}O$$

$$H_2O + {}^{\bullet}O \rightarrow 2{}^{\bullet}OH$$

As a result, the degradation of contaminants under sonophotocatalysis proceeds faster and the two effects are even synergistic.[112] Nevertheless, the application of ultrasound irradiation in photocatalytic water remediation, especially for emerging contaminants, is scarce. Its combination with photocatalysis has the potential to undoubtedly open up new opportunities in water treatment, at the expense of higher energy consumptions and possible catalyst film fouling.

Lessons learned and future steps

Catalytic tests have been often performed under unrealistic experimental conditions (*i.e.*, in terms of contaminant concentration, reaction time, effect of water pH, and influence of pre-existing ions. See Tables 4 and 5). Future studies need to be completed under more realistic experimental conditions, using the correct contaminant concentration indicated in Table 1, and exploring combination effects of multiple pollutants together. This will probably remain the only mode to validate the applicability of different nanotechnologies under comparable conditions. To the best of our knowledge, to date very few studies have explored catalytic effects on the removal of persistant viruses and bacteria in water.[163–165] These pathogens are creating an increasing number of health issues in many areas, and they will need to be taken under consideration in future studies. The long-term stability of most catalysts is largely unknown because most studies have been conducted for a relatively short period of time. Research addressing the long-term performance of water and wastewater treatment nanotechnologies is in great need. As a result, side-by-side comparison of nanotechnology-enabled systems and existing technologies is also fundamental.

Conclusions

In the Water Development Report 2019, the United Nations have highlighted that the availability of clean water is becoming a matter of major concern in the world, calling for the urgent implementation of new and less energy-intensive routes to purify wastewater. The emergence of advanced oxidation processes has provided a tool to remove organic pollutants and harmful pathogens from water, although it has been demonstrated that most of the catalysts and reactors used to date are unselective. This review has presented in a unified manner past and present technologies for the removal of pharmaceutical pollutants and for the catalytic recovery of CO_2 from it. It has shown that by tuning the materials property and the reactor nanoarchitecture, it is possible to increase the selectivity to the most thermodynamically stable CO_2 products. It has also highlighted current barriers and future research needs in the quest for processes that can selectively close the carbon cycle. Many of today's challenges include technical hurdles that can be tackled considering emerging aspects of catalyst and reactor design. Besides, to overcome barriers, collaborations between fundamental and applied disciplines, and the intersection of novel and diverse scientific areas will be essential in the years (and decades) to come.

Conflicts of interest

Nothing to declare.

References

1 UN-Water and The World Health Organization, *The United Nations World Water Development Report*, 2019.
2 J. R. Werber, C. O. Osuji and M. Elimelech, *Nat. Rev. Mater.*, 2016, **1**, 16018.
3 K. N. Heck, S. Garcia-Segura, P. Westerhoff and M. S. Wong, *Acc. Chem. Res.*, 2019, **52**, 906.

4 US Environmental Protection Agency, *Water Treatment Manual: Disinfection*, 2011.
5 T. Reemtsma, S. Weiss, J. Mueller, M. Petrović, S. Gonzalez, D. Barceló, F. Ventura and T. Knepper, *Environ. Sci. Technol.*, 2006, **40**, 5451.
6 J. Radjenović, M. Petrović and D. Barceló, *Trends Analyt. Chem.*, 2007, **26**, 1132.
7 H. L. Schoenfuss, E. T. Furlong, P. J. Phillips, T.-M. Scott, D. W. Kolpin, M. Cetkovic-Cvrlje, K. E. Lesteberg and D. C. Rearick, *Environ. Toxicol. Chem.*, 2016, **35**, 953.
8 T.-M. Scott, P. J. Phillips, D. W. Kolpin, K. M. Colella, E. T. Furlong, W. T. Foreman and J. L. Gray, *Sci. Total Environ.*, 2018, **636**, 69.
9 R. Loos, R. Carvalho, D. C. António, S. Comero, G. Locoro, S. Tavazzi, B. Paracchini, M. Ghiani, T. Lettieri, L. Blaha, B. Jarosova, S. Voorspoels, K. Servaes, P. Haglund, J. Fick, R. H. Lindberg, D. Schwesig and B. M. Gawlik, *Water Res.*, 2013, **47**, 6475.
10 E. L. Marron, W. A. Mitch, U. von Gunter and D. L. Sedlak, *Acc. Chem. Res.*, 2019, **52**, 615.
11 W. Rongwong, J. Lee, K. Goh, H. E. Karahan and T.-H. Bae, *npj Clean Water*, 2018, 21.
12 Y.-S. Jun, Y. Wu, D. Ghim, Q. Jiang, S. Cao and S. Singameneni, *Acc. Chem. Res.*, 2019, **52**, 1215.
13 M. Deborde and U. von Gunten, *Water Res.*, 2008, **42**, 13.
14 C. Wie, F. Zhang, Y. Hu, C. Feng and H. Wu, *Rev. Chem. Eng.*, 2016, 33, DOI: 10.1515/revce-2016-0008.
15 J. Schijven, P. Teunis, T. Suylen, H. Ketelaars, L. Hornstra and S. Rutjes, *Water Res.*, 2019, **158**, 34.
16 W. Yao, J. Fu, H. Yang, G. Yu and Y. Wang, *Water Res.*, 2019, **157**, 209.
17 X. Li, M. Cai, L. Wang, F. Niu, D. Yang and G. Zhang, *Sci. Total Environ.*, 2019, **659**, 1415.
18 European Cluster on Catalysis (ECC), *Science and Technology Roadmap on Catalysis for Europe*, 2016.
19 R. Andreozzi, V. Caprio, A. Insola and R. Marotta, *Catal. Today*, 1999, **53**, 51.
20 M. R. Hoffmann, S. T. Martin, W. Choi and D. W. Bahnemann, *Chem. Rev.*, 1995, **95**, 69.
21 M. Klavarioti, D. Mantzavinos and D. Kassinos, *Environ. Int.*, 2009, **34**, 402.
22 W. H. Glaze and J. W. Kang, *Ind. Eng. Chem. Res.*, 1989, **28**, 1573.
23 B. C. Hodges, E. L. Cates and J.-H. Kim, *Nat. Nanotechnol.*, 2018, **13**, 642.
24 M. Coto, S. C. Troughton, J. Duan, R. V. Kumar and T. W. Clyne, *Appl. Surf. Sci.*, 2018, **433**, 101.
25 B. E. Logan, *Environ. Sci. Technol. Lett.*, 2019, **6**, 511.
26 J. Coronas and J. Santamaría, *Catal. Today*, 1999, **51**, 377.
27 M. S. Hamdy, W. H. Saputera, E. J. Groenen and G. Mul, *J. Catal.*, 2014, **310**, 75.
28 M. A. Lazar, S. Varghese and S. S. Nair, *Catalysts*, 2012, **2**, 572.
29 A. K. Fard, G. McKay, A. Buekenhoudt and H. Al Sulaiti, *et al.*, *Materials*, 2018, **11**, 74.
30 P. Dong, X. Xi and G. Hou, Typical Non-TiO2-Based Visible-Light Photocatalysts, in *Semiconductor Photocatalysis: Materials, Mechanisms and Applications (Intech)*, 2016, ch. 8.
31 Z.-G. Zhao and M. Miyauchi, *Angew. Chem.*, 2008, **120**, 7159.
32 Y. Bi, S. Ouyang, N. Umezawa, J. Cao and J. Ye, *J. Am. Chem. Soc.*, 2011, **133**, 6490.
33 L. Zhang, D. Chen and X. Jiao, *J. Phys. Chem. B*, 2006, **110**, 2668.
34 M. C. Ortega-Liebana, J. L. Hueso, S. Ferdousi and R. Arenal, *et al.*, *Appl. Catal., B*, 2017, **218**, 68.
35 S. Álvarez-Torrellas, A. Rodríguez, G. Ovejero and J. García-Rodriguez, *Chem. Eng. J.*, 2016, **283**, 936.
36 Z. Jiang, Y. Liu, X. Sun, F. Tian, F. Sun, C. Liang, W. You, C. Han and C. Li, *Langmuir*, 2003, **19**, 731.
37 G. Vilé, D. Albani, M. Nachtegaal and Z. Chen, *et al.*, *Angew. Chem., Int. Ed.*, 2015, **54**, 11265.
38 T. S. Miller, A. B. Jorge, T. M. Suter and A. Sella, *et al.*, *Phys. Chem. Chem. Phys.*, 2017, **19**, 15613.
39 T. Torimoto, N. Nakamura, S. Ikeda and B. Ohtani, *Phys. Chem. Chem. Phys.*, 2002, **4**, 5910.
40 G. Xi, S. Ouyang and J. Ye, *Chem. – Eur. J.*, 2011, **17**, 9057.
41 Y. Xu and M. A. Schoonen, *Am. Mineral.*, 2000, **85**, 543.
42 X. Liu and K. L. Chen, *Environ. Sci.: Nano*, 2016, **3**, 146.
43 C. Wu, X. Zhao, Y. Ren, Y. Yue, W. Hua, Y. Cao, Y. Tang and Z. Gao, *J. Mol. Catal. A: Chem.*, 2005, **229**, 233.
44 T. Hasobe, Y. Kashiwagi, M. A. Absalom, J. Sly, K. Hosomizu, M. J. Crossley, H. Imahori, P. V. Kamat and S. Fukuzumi, *Adv. Mater.*, 2004, **16**, 975.
45 F. Wang, C. Di Valentin and G. Pacchioni, *ChemCatChem*, 2012, **4**, 476.
46 A. J. Cowan, C. J. Barnett, S. R. Pendlebury, M. Barroso, K. Sivula, M. Graetzel, J. R. Durrant and D. R. Klug, *J. Am. Chem. Soc.*, 2011, **133**, 10134.
47 X. Chang, T. Wang, P. Zhang, J. Zhang, A. Li and J. Gong, *J. Am. Chem. Soc.*, 2015, **137**, 8356.
48 A. Walsh, Y. Yan, M. N. Huda, M. M. Al-Jassim and S.-H. Wei, *Chem. Mater.*, 2009, **21**, 547.
49 W. Wang, M. O. Tadé and Z. Shao, *Chem. Soc. Rev.*, 2015, **44**, 5371.
50 D. J. Martin, G. Liu, S. J. Moniz, Y. Bi, A. M. Beale, J. Ye and J. Tang, *Chem. Soc. Rev.*, 2015, **44**, 7808.
51 H. Park, Y. K. Kim and W. Choi, *J. Phys. Chem. C*, 2011, **115**, 6141–6148.
52 X. Ma, Y. Lv, J. Xu, Y. Liu, R. Zhang and Y. Zhu, *J. Phys. Chem. C*, 2012, **116**, 23485.
53 V. Meille, *Appl. Catal., A*, 2006, **315**, 1.
54 A. Savateev, D. Dontsova, B. Kurpil and M. Antonietti, *J. Catal.*, 2017, **350**, 203.
55 C. Wang, X. Tan, J. Yan, B. Chai, J. Li and S. Chen, *Appl. Surf. Sci.*, 2017, **396**, 780.
56 J. Liu, B. He, Q. Chen, H. Liu, J. Li, Q. Xiong, X. Zhang, S. Yang, G. Yue and Q. H. Liu, *Electrochim. Acta*, 2016, **222**, 1677.
57 S. Indris, D. Bork and P. Heitjans, *J. Mater. Synth. Process.*, 2000, **8**, 245.

58 G. Vilé, S. Colussi, F. Krumeich, A. Trovarelli and J. Pérez-Ramírez, *Angew. Chem., Int. Ed.*, 2014, **53**, 12069.
59 R. Mehmood, X. Wang, P. Koshy, J. L. Yang and C. C. Sorrella, *CrystEngComm*, 2018, **20**, 1536.
60 S. Fernandez-Garcia, L. Jiang, M. Tinoco, A. B. Hungria, J. Han, G. Blanco, J. J. Calvino and X. Chen, *J. Phys. Chem. C*, 2016, **120**, 1891.
61 Z. Liu, X. Li, M. Mayyas, P. Koshy, J. N. Hart and C. C. Sorrell, *CrystEngComm*, 2018, **20**, 204.
62 M. Moser, G. Vilé, S. Colussi, F. Krumeich, D. Teschner, L. Szentmiklósi, A. Trovarelli and J. Pérez-Ramírez, *J. Catal.*, 2015, **331**, 128.
63 S. Akir, A. Barras, Y. Coffinier, M. Bououdina, R. Boukherroub and A. D. Omrani, *Ceram. Int.*, 2016, **42**, 10259.
64 A. Hui, J. Ma, J. Liu, Y. Bao and J. Zhang, *J. Alloys Compd.*, 2017, **696**, 639.
65 P. Dong, G. Hou, X. Xi, R. Shao and F. Dong, *Environ. Sci.: Nano*, 2017, **4**, 539.
66 Z. Wei, M. Endo-Kimura, K. Wang, C. Colbeau-Justin and E. Kowalska, *Nanomaterials*, 2019, **9**, 1447.
67 C. S. Bhatt, B. Nagaraj and A. K. Suresh, *J. Mol. Liq.*, 2017, **242**, 958.
68 M. Nolan, S. C. Parker and G. W. Watson, *Surf. Sci.*, 2005, **595**, 223.
69 T. X. T. Sayle, M. Cantoni, U. M. Bhatta, S. C. Parker, S. R. Hall, G. Mobus, M. Molinari, D. Reid, S. Seal and D. C. Sayle, *Chem. Mater.*, 2012, **24**, 1811.
70 J. Ge, Y. Zhang, Y.-J. Heo and S.-J. Park, *Catalysts*, 2019, **9**, 122.
71 C. Huang, C. Chen, M. Zhang, L. Lin, X. Ye, S. Lin, M. Antonietti and X. Wang, *Nat. Commun.*, 2015, **6**, 7698.
72 S. Ida, N. Kim, E. Ertekin, S. Takenaka and T. Ishihara, *J. Am. Chem. Soc.*, 2014, **137**, 239.
73 G. Liu, L. Z. Wang, H. G. Yang, H. M. Cheng and G. Q. Lu, *J. Mater. Chem.*, 2010, **20**, 831.
74 L. G. Devi, N. Kottam, B. N. Murthy and S. G. Kumar, *J. Mol. Catal. A: Chem.*, 2010, **328**, 44.
75 R. Asahi, T. Morikawa, H. Irie and T. Ohwaki, *Chem. Rev.*, 2014, **114**, 9824.
76 N. Salah, A. Hameed, M. Aslam, M. S. Abdel-Wahab, S. S. Babkair and F. S. Bahabri, *Chem. Eng. J.*, 2016, **291**, 115.
77 E. B. Simsek, *Appl. Catal., B*, 2017, **200**, 309.
78 H. Labiadh, T. B. Chaabane, L. Balan, N. Becheik, S. Corbel, G. Medjahdi and R. Schneider, *Appl. Catal., B*, 2014, **144**, 29.
79 J. Wang, Q. Zhang, F. Deng, X. Luo and D. D. Dionysiou, *Chem. Eng. J.*, 2020, **379**, 122264.
80 Y. Chen and X. Bai, *Catalysts*, 2020, **10**, 142.
81 H. Li, Y. Li, L. Xiang, Q. Huang, J. Qiu, H. Zhang, M. Venkat, F. Baron, J. Barrault, S. Petit and S. Valange, *J. Hazard. Mater.*, 2015, **287**, 32.
82 R. Greco, W. Goessler, D. Cantillo and C. O. Kappe, *ACS Catal.*, 2015, **5**, 1303.
83 A. Visan, J. R. van Ommen, M. T. Kreutzer and R. G. H. Lammertink, *Ind. Eng. Chem. Res.*, 2019, **58**, 5349.
84 G. Vilé, S. Richard-Bildstein, A. Lhuillery and G. Rueedi, *ChemCatChem*, 2018, **10**, 3786.
85 D. K. Lee, S. C. Kim, I. C. Cho, S. J. Kim and S. W. Kim, *Sep. Purif. Technol.*, 2004, **34**, 59.
86 H. Zhao, S. Xu, J. Zhong and X. Bao, *Catal. Today*, 2004, **93–95**, 857.
87 A. E. Palomares, C. Franch and A. Corma, *Catal. Today*, 2010, **149**, 348.
88 N. A. Hamill, L. R. Weatherley and C. Hardacre, *Appl. Catal., B*, 2001, **30**, 49.
89 A. R. Khataee, M. Fathinia and S. Aber, *Ind. Eng. Chem. Res.*, 2010, **49**, 12358.
90 A. Petala, D. Spyrou, Z. Frontistis, D. Mantzavinos and D. I. Kondarides, *Catal. Today*, 2019, **328**, 223.
91 L. Amini-Rentsch, E. Vanoli, S. Richard-Bildstein, R. Marti and G. Vilé, *Ind. Eng. Chem. Res.*, 2019, **58**, 10164.
92 S. Tortoioli, A. Friedli, A. Prud'homme, S. Richard-Bildstein, P. Kohler, S. Abele and G. Vilé, *Green Chem.*, 2020, **22**, 3748.
93 K. S. Ochoa-Gutiérrez, E. Tabares-Aguilar, M. Á. Mueses, F. Machuca-Martínez and G. Li Puma, *Chem. Eng. J.*, 2018, **341**, 628.
94 G. E. Imoberdorf, A. E. Cassano, O. M. Alfano and H. A. Irazoqui, *AIChE J.*, 2006, **52**, 1814.
95 D. Albani, G. Vilé, M. A. B. Toro, R. Kaufmann, S. Mitchell and J. Pérez-Ramírez, *React. Chem. Eng.*, 2016, **1**, 454.
96 M. U. Azam, M. Tahir, M. Umer, M. M. Jaffar and M. G. M. Nawawi, *Appl. Surf. Sci.*, 2019, **484**, 1089.
97 K. C. Lee, H. J. Beak and K. H. Choo, *Water Res.*, 2015, **86**, 58.
98 P. Kumari, N. Bahadur and L. F. Dumée, *Sep. Purif. Technol.*, 2020, **230**, 115878.
99 R. Molinari, C. Lavorato and P. Argurio, *Catal. Today*, 2017, **281**, 144.
100 B. M. Esteves, C. S. D. Rodrigues and L. M. Madeira, Applications of Advanced Oxidation Processes (AOPs) in Drinking Water Treatment, in *The Handbook of Environmental Chemistry (HEC)*, 2017, vol. 67.
101 Y. Boyjoo, H. Sun, J. Liu, V. K. Pareek and S. Wang, *Chem. Eng. J.*, 2017, **310**, 537.
102 P. Kumari, N. Bahadur and L. F. Dumée, *Sep. Purif. Technol.*, 2020, **230**, 115878.
103 D. Lee, P. Hacarlioglu and S. T. Oyama, *Top. Catal.*, 2004, **29**, 45.
104 N. Jallouli, L. M. Pastrana-Martinez, A. R. Ribeiro, N. F. F. Moreira, J. L. Faria, O. Hentati, A. M. T. Silva and M. Ksibi, *Chem. Eng. J.*, 2018, **334**, 976.
105 W. Zhang, L. Ding, J. Luo, M. Y. Jaffrin and B. Tang, *Chem. Eng. J.*, 2016, **302**, 446.
106 J. R. Domínguez, T. González, P. Palo and E. M. Cuerda-Correa, *Desalination*, 2011, **269**, 231.
107 R. Comparelli, E. Fanizza, M. L. Curri, P. D. Cozzoli, G. Mascolo and A. Agostiano, *Appl. Catal., B*, 2005, **60**, 1.
108 H. Lu, Z. Zhu, H. Zhang, J. Zhu, Y. Qiu, L. Zhu and S. Küppers, *ACS Appl. Mater. Interfaces*, 2016, **8**, 25343.
109 J. Carbajo, M. Jimenez, S. Miralles, S. Malato, M. Faraldos and A. Bahamonde, *Chem. Eng. J.*, 2016, **291**, 64.

110 C. Wu, L. Lu, A.-Z. Peng, G.-K. Jia, C. Peng, Z. Cao, Z. Tang, W.-M. He and X. Xu, *Green Chem.*, 2018, **20**, 3683.
111 M. Manzoli and B. Bonelli, *Catalysts*, 2018, **8**, 262.
112 A. Biswas, S. Saha and N. R. Jana, *ACS Appl. Nano Mater.*, 2019, **2**, 1120.
113 D. S. Francy, E. A. Stelzer, R. N. Bushon, A. M. G. Brady, B. E. Mailot, S. K. Spencer, M. A. Borchardt, A. G. Elber, K. R. Riddell and T. M. Gellner, *Quantifying Viruses and Bacteria in Wastewater - Results, Interpretation Methods, and Quality Control*, U.S. Department of the Interior & U.S. Geological Survey, 2011.
114 European Environment Agency, *Industrial Waste Water Treatment - Pressures on Europe's Environment*, 2018.
115 European Union, *EU Wide Monitoring Survey on Waste Water Treatment Plant Effluents*, 2012.
116 W. J. Lodder and A. M. de Roda Husman, *Appl. Environ. Microbiol.*, 2005, **71**, 1453.
117 F. G. Masclaux, P. Hotz, D. Gashi, D. Savova-Bianchi and A. Oppliger, *Environ. Res.*, 2014, **133**, 260.
118 T. A. Kurniawan, L. Yanyan, T. Ouyang, A. B. Albadarin and G. Walker, *Mater. Sci. Semicond. Process.*, 2018, **73**, 42.
119 L. Yanyan, T. A. Kurniawan, Z. Ying, A. B. Albadarin and G. Walker, *J. Mol. Liq.*, 2017, **243**, 761.
120 M. G. D. de Luna, J. C. Lin, M. J. N. Te-Gotostos and M. C. Lu, *Sustainable Environ. Res.*, 2016, **26**, 161.
121 A. Hassani, A. Khataee, S. Karaca and M. J. Fathinia, *J. Environ. Chem. Eng.*, 2017, **5**, 1964.
122 A. Surenjan, B. Sambandam, T. Pradeep and L. Philip, *J. Environ. Chem. Eng.*, 2017, **5**, 757.
123 Y. An, D. J. de Ridder, C. Zhao, K. Schoutteten, J. Vanden Bussche, H. Zheng, G. Chen and L. Vanhaecke, *Water Sci. Technol.*, 2016, **73**, 2868.
124 D. Kanakaraju, C. A. Motti, B. D. Glass and M. Oelgemöller, *Environ. Sci. Pollut. Res.*, 2016, **23**, 17437.
125 A. Kumar, M. Khan, X. Zeng and I. M. C. Lo, *Chem. Eng. J.*, 2018, **353**, 645.
126 L. Lin, H. Wang and P. Xu, *Chem. Eng. J.*, 2017, **310**, 389.
127 N. Jallouli, L. M. Pastrana-Martínez, A. R. Ribeiro, N. F. F. Moreira, J. L. Faria, O. Hentati, A. M. T. Silva and M. Ksibi, *Chem. Eng. J.*, 2018, **334**, 976.
128 T. Huyen, T. Chi, N. Dung, H. Kosslick and N. Liem, *Nanomaterials*, 2018, **8**, 276.
129 L. Djouadia, H. Khalafa, H. Boukhatemab, H. Boutoumia, A. Kezzimec, J. A. Santaballad and M. Canle, *Appl. Clay Sci.*, 2018, **166**, 27–37.
130 C. Martínez, S. Vilariño, M. I. Fernández, J. Faria, M. L. Canle and J. A. Santaballa, *Appl. Catal., B*, 2013, **142–143**, 633.
131 J. Suave, S. M. Amorim and R. F. P. M. Moreira, *J. Environ. Chem. Eng.*, 2017, **5**, 3215.
132 M. A. Sousa, C. Gonçalves, V. J. P. Vilar, R. A. R. Boaventura and M. F. Alpendurada, *Chem. Eng. J.*, 2012, **198–199**, 301.
133 C.-S. Kuo, C.-F. Lin and P.-K. A. Hong, *J. Hazard. Mater.*, 2016, **301**, 137.
134 M. Antonopoulou and I. Konstantinou, *Appl. Catal., A*, 2016, **515**, 136.
135 X. Zheng, S. Xu, Y. Wang, X. Sun, Y. Gao and B. Gao, *J. Colloid Interface Sci.*, 2018, **527**, 202.
136 Y. Gan, Y. Wei, J. Xiong and G. Cheng, *Chem. Eng. J.*, 2018, **349**, 1.
137 M. Khodadadi, M. H. Ehrampoush, M. T. Ghaneian, A. Allahresani and A. H. Mahvi, *J. Mol. Liq.*, 2018, **255**, 224.
138 M. Ahmadi, H. R. Motlagh, N. Jaafarzadeh, A. Mostoufi, R. Saeedi, G. Barzegar and S. Jorfi, *J. Environ. Manage.*, 2017, **186**, 55.
139 S. Oros-Ruiz, R. Zanella and B. Prado, *J. Hazard. Mater.*, 2013, **263**, 28.
140 A. Gholami, M. Hajiani, M. Hossein and S. Anari, *J. Water Environ. Nanotechnol.*, 2019, **4**, 139.
141 M. N. Abellán, B. Bayarri, J. Giménez and J. Costa, *Appl. Catal., B*, 2007, **74**, 233.
142 J. R. Kim and E. Kan, *J. Environ. Manage.*, 2016, **180**, 94.
143 M. Długosz, P. Żmudzki, A. Kwiecień, K. Szczubiałka, J. Krzek and M. Nowakowska, *J. Hazard. Mater.*, 2015, **298**, 146.
144 S. Yu, Y. Wang, F. Sun, R. Wang and Y. Zhou, *Chem. Eng. J.*, 2018, **337**, 183.
145 H. Gong and W. Chu, *J. Hazard. Mater.*, 2016, **314**, 197.
146 A. Hu, X. Zhang, K. D. Oakes, P. Peng, Y. N. Zhou and M. R. Servos, *J. Hazard. Mater.*, 2011, **189**, 278.
147 P. Calza, C. Hadjicostas, V. A. Sakkas, M. Sarro, C. Minero, C. Medana and T. A. Albanis, *Appl. Catal., B*, 2016, **183**, 96.
148 P. Chen, F. Wang, Z.-F. Chen, Q. Zhang, Y. Su, L. Shen, K. Yao, Y. Liu, Z. Cai, W. Lv and G. Liu, *Appl. Catal., B*, 2017, **204**, 250.
149 R. Molinari, A. Caruso, P. Argurio and T. Poerio, *J. Membr. Sci.*, 2008, **319**, 54.
150 M. Akkari, P. Aranda, C. Belver, J. Bedia, A. Ben Haj Amara and E. Ruiz-Hitzky, *Appl. Clay Sci.*, 2018, **156**, 104.
151 I. A. Pronin, N. V. Kaneva, A. S. Bozhinova, I. A. Averin, K. I. Papazova and D. T. Dimitrov, *Kinet. Catal.*, 2014, **55**, 167.
152 J. Zhu, Z. Zhu, H. Zhang, H. Lu, W. Zhang, Y. Qiu, L. Zhu and S. Küppers, *Appl. Catal., B*, 2018, **225**, 550.
153 J. Sun, Y. Guo, Y. Wang, D. Cao, S. Tian, K. Xiao, R. Mao and X. Zhao, *Chem. Eng. J.*, 2018, **332**, 312.
154 J. Bohdziewicz, E. Kudlek and M. Dudziak, *Desalin. Water Treat.*, 2016, **57**, 1552.
155 H. Shao, X. Zhao, Y. Wang, R. Mao, Y. Wang, M. Qiao, S. Zhao and Y. Zhu, *Appl. Catal., B*, 2017, **218**, 810.
156 G. Di, Z. Zhu, H. Zhang, J. Zhu, H. Lu, W. Zhang, Y. Qiu, L. Zhu and S. Küppers, *Chem. Eng. J.*, 2017, **328**, 141.
157 J. Choina, A. Bagabas, C. Fischer, G. U. Flechsig, H. Kosslick and A. Alshammari, *et al.*, *Catal. Today*, 2015, **241**, 47.
158 G. Xu, M. Li, Y. Wang, N. Zheng, L. Yang, H. Yu and Y. Yu, *Sci. Total Environ.*, 2019, **678**, 173.
159 M. Karaca, M. Kirans, S. Karaca, A. Khataee and A. Karimi, *Ultrason. Sonochem.*, 2016, **31**, 250.
160 H. Chen, B. Gao and H. Li, *J. Hazard. Mater.*, 2015, **282**, 201.

161 F. Deng, F. Zhong, D. Lin, L. Zhao, Y. Liu, J. Huang, X. Luo, S. Luo and D. D. Dionysiou, *Appl. Catal., B*, 2017, **219**, 163.
162 X. Wang, J. Jia and Y. Wang, *Chem. Eng. J.*, 2017, **315**, 274.
163 M. Farzadkia, K. Rahmani, M. Gholami, A. Esrafili, A. Rahmani and H. Rahmani, *Korean J. Chem. Eng.*, 2014, **31**, 2014.
164 X. Gao, W. Peng, G. Tang, Q. Guo and Y. Luo, *J. Alloys Compd.*, 2018, **757**, 455.
165 N. Davari, M. Farhadian, A. R. S. Nazar and M. Homayoonfal, *J. Environ. Chem. Eng.*, 2017, **5**, 5707.
166 A. Mirzaei, Z. Chen, F. Haghighat and L. Yerushalmi, *Sustain. Cities Soc.*, 2016, **27**, 407.